Peak effect due to Josephson vortices in superconducting $Pr_{0.88}LaCe_{0.12}CuO_{4-\delta}$ single crystals

Yue Wang,[1] Cong Ren,[1] Lei Shan,[1] Shiliang Li,[2] Pengcheng Dai,[2,3] and Hai-Hu Wen[1,*]

[1]*National Laboratory for Superconductivity, Institute of Physics and Beijing National Laboratory for Condensed Matter Physics, Chinese Academy of Sciences, P.O. Box 603, Beijing 100080, People's Republic of China*

[2]*Department of Physics and Astronomy, The University of Tennessee, Knoxville, Tennessee 37996-1200, USA*

[3]*Center for Neutron Scattering, Oak Ridge National Laboratory, Oak Ridge, Tennessee 37831-6393, USA*

(Received 5 July 2006; revised manuscript received 1 February 2007; published 6 April 2007)

We have measured ac magnetic susceptibility ($\chi=\chi'+i\chi''$) of the electron-doped superconducting $Pr_{0.88}LaCe_{0.12}CuO_{4-\delta}$ with applied magnetic field (H) either parallel or perpendicular to the CuO_2 plane ($H\|ab$-plane or $H\|c$-axis). For $H\|ab$-plane, a peak in the temperature dependence of the screening current is revealed as a dip in the real part of the ac susceptibility χ. The temperature at which this peak anomaly occurs decreases with increasing field and lies well below the irreversibility line in the H-T phase diagram. This peak effect may arise from the phase transition of Josephson vortices from a quasiordered vortex lattice to a disordered glass phase.

DOI: 10.1103/PhysRevB.75.134505 PACS number(s): 74.25.Qt, 74.72.Jt, 74.25.Sv

I. INTRODUCTION

Determining the magnetic phase diagram of the vortex lattice in type-II superconductors is important because of its potential technical applications. In the mixed state, the critical current density J_c or the magnetization, instead of decreasing monotonically, may go through a maximum and thus exhibit a peak feature with increasing temperature T or magnetic field H. Many experimental and theoretical efforts have been carried out to understand the underlying mechanism of this anomalous phenomenon.

The peak effect has been observed in various superconductors, including conventional superconductors such as MgB_2 (Ref. 1) and high-T_c cuprates. In low-T_c conventional superconductors such as Nb,[2] 2H-$NbSe_2$,[3,4] and $CeRu_2$,[5] it generally appears at H near the upper critical field $H_{c2}(T)$. In high-T_c copper oxide $Bi_2Sr_2CaCu_2O_{8+\delta}$ (Bi2212),[6] a sharp increase in magnetization with increasing H, as the onset of the peak anomaly, has been observed in isothermal magnetization hysteresis loops. This so-called second peak, which occurs well below the irreversibility field $H_{irr}(T)$ at low temperature, is also mapped as the fishtail peak in $YBa_2Cu_3O_{7-\delta}$ (YBCO) crystals.[7] In a pure YBCO crystal,[8] a giant peak effect in the ac susceptibility has been reported and interpreted as the signature of a vortex-lattice melting transition.

It is generally believed that the vortex phase diagram is governed by the interplay between three energy scales: the vortex elastic energy E_{el}, the thermal fluctuation energy E_{th} and the pinning energy E_{pin}.[9] Although the roles of these basic energies in producing the peak effect have been discussed,[10] it is difficult to separate individual effects in some materials.[4] The electron-doped cuprates $R_{2-x}Ce_xCuO_{4-\delta}$ (R=La,Pr,Nd), as a small family of high-T_c superconductors, have relatively lower transition temperatures ($T_c\sim 25$ K) than the hole-doped cuprates ($T_c\sim 90$ K for YBCO). Using the material parameters of the $Nd_{2-x}Ce_xCuO_{4-\delta}$ (NCCO),[11] the Ginzburg number $Gi=(T_c/H_c^2\xi_c\xi_{ab}^2)^2/2$, where H_c, ξ_{ab}, and ξ_c are the thermodynamic critical field, the coherence length in ab-plane and along c-axis at $T=0$, respectively,[9] a measure of the thermal fluctuations, is estimated to be 10^{-3} which is lower than many other cuprates (10^{-2} for YBCO). This implies a less significant role for E_{th} in NCCO, which was indeed demonstrated in previous local magnetic measurements[12] where the onset of the second peak was discussed as due to the competition between the E_{pin} and E_{el} and the contribution of E_{th} was ignored. Since superconducting NCCO has $(Nd,Ce)_2O_3$ as a impurity phase which can be polarized by an applied field,[13] it is clearly interesting to explore the vortex matter in electron-doped superconducting $Pr_{0.88}LaCe_{0.12}CuO_{4-\delta}$ (PLCCO) where the cubic impurity phase $(Pr,La,Ce)_2O$ has a nonmagnetic ground state[14] and therefore will not influence the vortex lattice.

Most previous measurements showing the peak effect in high-T_c superconductors were performed for $H\|c$-axis, i.e., H perpendicular to the CuO_2 layers. The vortex matter forms a lattice of stacks of pancake vortices in this field configuration, whereas it forms a lattice of Josephson vortices when the applied field is parallel to the layers ($H\|ab$-plane).[9] In high-T_c cuprates, due to the anisotropy and the underlying layered structure, Josephson vortices are stretched strongly and separated by a large distance along the layers. Consequently, the lattice of Josephson vortices becomes deformed compared with the regular-triangle lattice of pancake vortices. Another characteristic of Josephson vortices is the presence of intrinsic pinning.[15] The periodic modulation of the order parameter along the c axis tends to confine Josephson vortices to the region between two neighboring CuO_2 planes in order to reduce the loss of the superconducting cohesive energy, and thus works as a nonrandom source of intrinsic pinning. These new features offer possibilities for behavior in the phases and phase transitions of Josephson vortices.

In this paper, we present a study of the ac magnetic response in a PLCCO single crystal, which, as a sister of the NCCO, is another highly anisotropic electron-doped cuprate superconductor (anisotropy ratio $\varepsilon\sim 1/20$).[16] The susceptibility is found to show qualitatively different features between $H\|ab$-plane and $H\|c$-axis. For $H\|ab$-plane we find the peak effect due to Josephson vortices. It appears at lower temperature with increasing dc field and the characteristic

line of the peak effect is located far below the irreversibility line in the vortex *H-T* phase diagram. The peak effect may arise from a disorder-induced transition in the solid phase of the Josephson vortex matter.

II. EXPERIMENTAL DETAILS

The high quality PLCCO single crystal was grown by the traveling solvent floating zone method. It has a mass of 6.58 mg and a bar shape with dimensions $0.86\times0.70\times1.76$ mm^3 (the c axis along the longest dimension). By using a Quantum Design superconducting quantum interference device (SQUID) magnetometer, the sample was characterized by dc magnetization at 10 Oe parallel to the *ab*-plane (zero field cooled), showing a sharp superconducting transition with a critical temperature $T_c\approx23.5$ K. This indicates a homogeneity of the sample along the c axis.

The ac susceptibility $\chi=\chi'+i\chi''$ was measured with the mutual inductance technique using the MP (magnetic properties) probe of an Oxford-MaglabEXA-12 cryogenic system. In this paper the main results were obtained with both ac and dc fields applied parallel to the *ab*-plane of the crystal. For comparison the susceptibility with fields parallel to the c axis is also presented. For each measurement, the dc field was applied above T_c and then the sample was cooled to the lowest desired temperature without any applied ac field, and finally the ac field was superimposed and data were recorded in the warming process. Most of the curves were obtained at a sweeping rate of 0.3 K/min.

III. RESULTS AND DISCUSSION

A. Comparison between $H\|ab$-plane and $H\|c$-axis

We first determine the behavior of the ac response in PLCCO. In general, the real part of the ac susceptibility (χ') is a measure of the screening properties of the sample and the imaginary part (χ'') measures the energy dissipation. For type-II superconductors, the dissipation mechanism in the ac response may be viscous flux flow or hysteresis due to the pinning of flux lines. The former may be treated in a linear diffusive model[17] which shows that χ depends on the frequency f but not on the amplitude h of the ac field, whereas the latter can be described in a critical state model[18] predicting an amplitude dependent but frequency independent ac susceptibility. By measuring the h and f dependence of the ac susceptibility, we can determine different contributions to the vortex dynamics.

Figure 1 shows $\chi(T)$ at various h and f of $H_{ac}\|ab$-plane in zero dc field. Susceptibility $\chi(T)$ at $f=333$ Hz depends strongly on the amplitude of H_{ac} [Fig. 1(a)]. At $h=1$ Oe, the ac susceptibility gives a $T_c\approx23.8$ K (upper onset of χ'' peak), similar to the dc magnetization result. As h increases, χ' shows a broad transition and its low temperature part shifts upward corresponding to a decrease in the screening current. At the same time, the peak of χ'' becomes wider and shifts to lower T and its height increases. Note that the dissipation is still appreciable even down to $T=2$ K at $h=15$ Oe. These features clearly characterize a nonlinear response of the sample under the measured condition. On the other hand, $\chi(T)$ is almost independent on the frequency, as depicted in Figs. 1(b)–1(d) where χ vs T with varying f at fixed amplitude $h=1$, 5, and 10 Oe are shown, respectively. This frequency independence of $\chi(T)$, together with its strongly amplitude dependence, indicates that the ac response for $H\|ab$-plane is consistent with the critical state model.

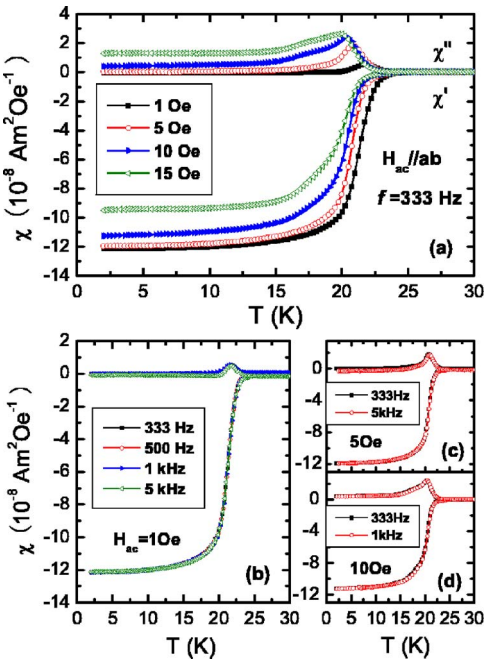

FIG. 1. (Color online) Temperature dependence of the ac susceptibility $\chi=\chi'+i\chi''$ for $H_{ac}\|ab$-plane at different h and f ($H_{dc}=0$ T). (a) Variation of h from 1 Oe to 15 Oe at fixed $f=333$ Hz. (b) Variation of f from 333 Hz to 5 kHz at $h=1$ Oe. (c) $f=333$ and 5 kHz, $h=5$ Oe. (d) $f=333$ and 1 kHz, $h=10$ Oe.

Figure 2 and 3 show the ac response of the sample for $H\|c$-axis in zero and nonzero dc fields, respectively. Let us first see the susceptibility at various H_{ac} in $H_{dc}=0$ T. Figure 2(a) is the plot of $\chi(T)$ at different amplitudes, $f=333$ Hz. With increasing h, in the vicinity of the superconducting transition there is a weak shift of the curve to lower temperature, but the width of the transition in χ' remains almost unchanged. The χ'' peaks are still symmetric and the peak heights are the same for h varied from 5 Oe to 30 Oe. Shown in Fig. 2(b) is the frequency dependence of $\chi(T)$ at $h=10$ Oe. The curve moves slightly to higher temperature as f increases in the range measured. These features are qualitatively different from those shown for $H\|ab$-plane and suggest that the response of the crystal for $H\|c$-axis is more close to the flux flow regime, though the amplitude dependence of $\chi(T)$ near T_c may relate to some thermal activated processes.[19] Another prominent difference between $H\|ab$-plane and $H\|c$-axis, revealed in Fig. 2, is that for $H\|c$-axis at low temperature the sample maintains full flux expulsion and thus exhibits a completely linear response up to $h=30$ Oe. The appearance of nonlinear response at lower ac fields for $H\|ab$-plane may partly arise from the presence of intrinsic pinning due to CuO_2 planes.

Shown in Fig. 3(a) is the $\chi(T)$ for $H\|c$-axis at different H_{ac} in $H_{dc}=0.05$ T. We see its variation with h is similar to

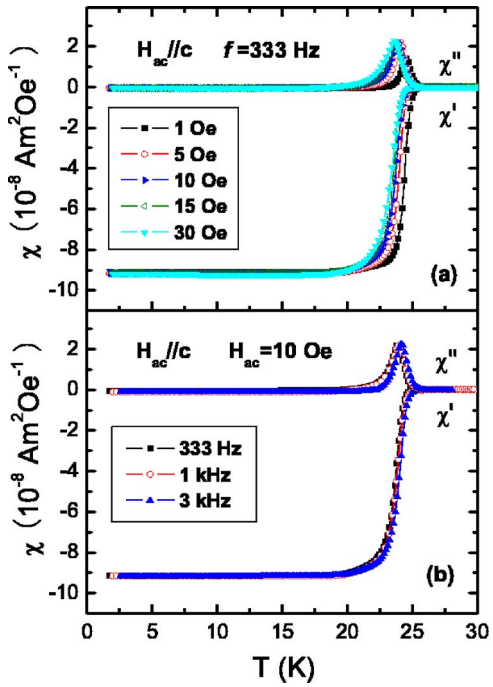

FIG. 2. (Color online) Temperature dependence of the ac susceptibility $\chi=\chi'+i\chi''$ for $H_{ac}\|c$-axis at different h and f ($H_{dc}=0$ T). (a) Variation of h from 1 Oe to 30 Oe at fixed $f=333$ Hz. (b) Variation of f from 333 Hz to 3 kHz at $h=10$ Oe.

the one presented in Fig. 2(a) for $H_{dc}=0$ T. In particular, it also shows the amplitude independence at low T, indicating again a linear response of the sample in this temperature range. In Fig. 3(b) are the curves at $H_{ac}=30$ Oe with H_{dc} ranging from 0 T to 0.3 T. When increasing the dc field, the superconducting transition shifts parallel to lower temperature with no pronounced broadening, which, resembling the behavior in conventional type-II superconductors, is analogous to the observation in measurements at $H_{ac}=1$ Oe (not shown).

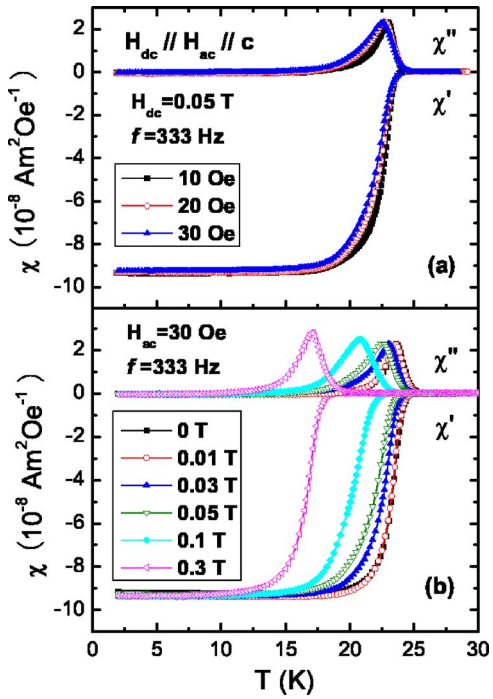

FIG. 3. (Color online) Temperature dependence of the ac susceptibility $\chi=\chi'+i\chi''$ for $H_{dc}\|H_{ac}\|c$-axis. (a) $H_{ac}=10$, 20 and 30 Oe, $f=333$ Hz at $H_{dc}=0.05$ T. (b) Variation of H_{dc} up to 0.3 T at $H_{ac}=30$ Oe, $f=333$ Hz.

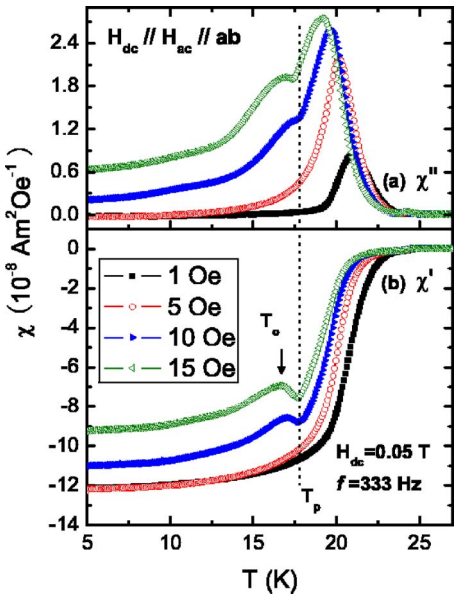

FIG. 4. (Color online) Temperature dependence of the ac susceptibility χ'' [in (a)] and χ' [in (b)] for different H_{ac} at $f=333$ Hz, $H_{dc}=0.05$ T ($H\|ab$-plane). At high h the peak effect is presented as a dip in $\chi'(T)$ at the peak temperature T_p. The marked arrow in (b) denotes the onset temperature T_o of the peak effect at $H_{ac}=15$ Oe.

B. Peak effect for $H\|ab$-plane

In this part, unless otherwise specified, the presented data and relating discussion are all for $H\|ab$-plane, i.e., $H_{dc}\|H_{ac}\|ab$-plane, with H_{ac} fixed at $f=333$ Hz. Figure 4 shows $\chi(T)$ in $H_{dc}=0.05$ T for different amplitudes of H_{ac}. When h increases to 10 Oe, χ' shows a dip in its temperature dependence and a shoulder forms in χ'' on its original peak structure. Similar effect happens at $h=15$ Oe, except that the shoulder in $\chi''(T)$ evolves into an additional small peak. This dip feature in $\chi'(T)$, as a well-established signature of the peak effect,[20–22] manifests its existence in PLCCO for $H\|ab$-plane. In the critical state model, the screening current in the sample is the J_c and both ac field and current penetrate to a depth $L_p \propto h/J_c$. Moreover, χ is a function of the ratio of L_p to the characteristic dimension of the sample.[23] Therefore, the measurement of χ is essentially equivalent to a measurement of J_c. Particularly, a numerical approximation gives $\chi'=-\pi J_c d/h$ (in cgs), where d is the width of the sample.[20] So the dip in $\chi'(T)$ signifies a peak in $J_c(T)$ and namely the presence of peak effect. We note that, for $H_{dc}\|H_{ac}\|ab$-plane, the peak effect was also observed in a less anisotropic $YBa_2Cu_3O_{6.55}$ single crystal.[22]

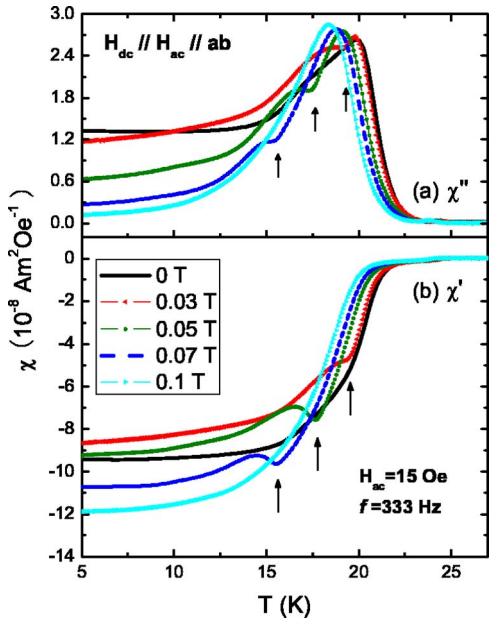

FIG. 5. (Color online) Temperature dependence of the ac susceptibility χ'' [in (a)] and χ' [in (b)] for different H_{dc} at $H_{ac}=15$ Oe, $f=333$ Hz ($H\|ab$-plane). The arrows denote the T_p for different dc fields [in (b)] and the corresponding shoulders in $\chi''(T)$ [in (a)].

As shown in Fig. 4(b), the peak temperature T_p, corresponding to the dip in $\chi'(T)$, is nearly independent on the ac field amplitude. At $h=10$ and 15 Oe, the T_p are 17.76 K and 17.63 K, respectively. The slight decrease of T_p for $h=15$ Oe arises from the drop in T_p with increasing the total field $H_{dc}+H_{ac}$. However, the onset temperature T_o of the peak effect varies with h. $T_o=17.14$ K and 16.57 K at $h=10$ Oe and 15 Oe in turn. In accordance with $\chi'(T)$, $\chi''(T)$ shows a slow down of the increasing rate in dissipation at $h=10$ Oe or even a decrease in dissipation at $h=15$ Oe between temperature T_o and T_p. This can be seen more clearly in the differential curve of $\chi''(T)$ and suggests a change in governing the losses in the sample.

We note that no peak effect is detected at low ac field amplitudes. In YBCO crystals, similar behavior is also reported.[24] Though overall responses of the sample agree with the critical state model, this may indicate that a bulk critical state is not formed in PLCCO below T_p at low h. When the H_{ac} is small enough, the screening current generated in the sample may be lower than the J_c for temperatures around T_p and, as a consequence, one is prohibited to detect the peak effect in $J_c(T)$. For $H\|c$-axis, it should be reminded that though the second peak has been revealed in isothermal magnetization hysteresis loops in NCCO,[12,25,26] no peak effect is observed in PLCCO at comparable field and temperature range in the ac susceptibility at $H_{ac}=30$ Oe, as shown in Fig. 3(b).

Figure 5 illustrates how the peak effect varies as the dc field increases for $H_{ac}=15$ Oe. Similar results were obtained for $H_{ac}=10$ Oe. The T_p and the corresponding shoulders in $\chi''(T)$ are denoted by arrows in Fig. 5(b) and Fig. 5(a), respectively. A general trend of decreasing T_p with increasing field is clearly seen. In $H_{dc}=0.03$ T, the peak effect is depicted actually as a kink in $\chi'(T)$. At low temperature below T_p, an enhancement of the diamagnetism of the sample, accompanied by a decrease in dissipation, is demonstrated when the dc field increases, which is consistent with the common belief that the effective disorder, served as the pinning center, increases upon raising the field. Note that up to $H_{dc}=0.1$ T, the peak effect is no longer observed and the crystal shows strongest diamagnetism and lowest dissipation at low T.

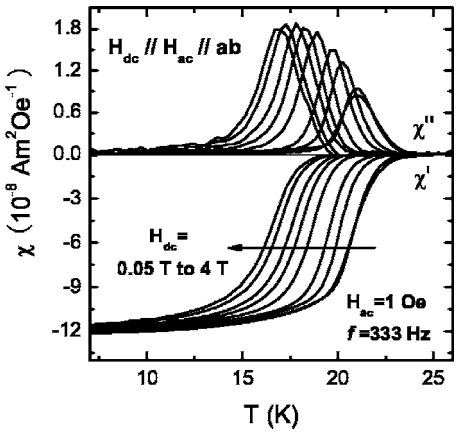

FIG. 6. $\chi(T)$ for various H_{dc} at $H_{ac}=1$ Oe, $f=333$ Hz ($H\|ab$-plane). $H_{dc}=0.05$, 0.1, 0.3, 0.5, 1, 1.5, 2, 3, and 4 T (from right to left).

To understand the underlying physics of the peak effect, we also performed the ac measurement to determine the irreversibility line, which, marking the line of $J_c=0$, is another pinning-related phenomenon in the vortex matter. Figure 6 shows $\chi(T)$ for various H_{dc} at $H_{ac}=1$ Oe. The irreversibility temperature T_{irr} was defined by the onset of the diamagnetic signal in $\chi'(T)$. This determination is common in ac susceptibility and is equivalent to find the upper onset of the $\chi''(T)$ peak.[19] By extracting the temperature where $\chi'(T)$ becomes zero at each H_{dc} in Fig. 6, we obtain the T_{irr} at various H_{dc}, i.e., the irreversibility line in PLCCO.

Figure 7 shows the experimental irreversibility points T_{irr} and the peak temperatures T_p in the H-T plane in a semilog plot. Here, the T_{irr} points for $H\|c$-axis are also plotted. They are determined from $\chi(T)$ at $H_{ac}=1$ Oe with $H_{dc}\|H_{ac}\|c$-axis, analogous to the points for $H\|ab$-plane. The dashed and dotted lines in the figure are fits to T_{irr} using the empirical formulas $H_{irr}(T)=88[1-(T/T_c)^2]^{3.9}$ and $H_{irr}(T)=5.4(1-T/T_c)^{2.2}$ with $T_c=25$ K for $H\|ab$-plane and $H\|c$-axis, respectively. A theoretical fit to T_p we shall discuss later is also shown as a solid line. For $H\|ab$-plane, it is apparent that the line of T_p locates well below the T_{irr} line.

Among many microscopic mechanisms for the peak effect, models including a dimensional crossover (3D-2D) in the vortex structure[27] and thermal-disorder induced vortex pancake decoupling transition[28] were developed considering $H\|c$-axis and the interlayer decoupling of the pancake vortices. These models are inappropriate to account for the present result since we are dealing with an array of Josephson vortices. Similarly, a matching effect between the vortex

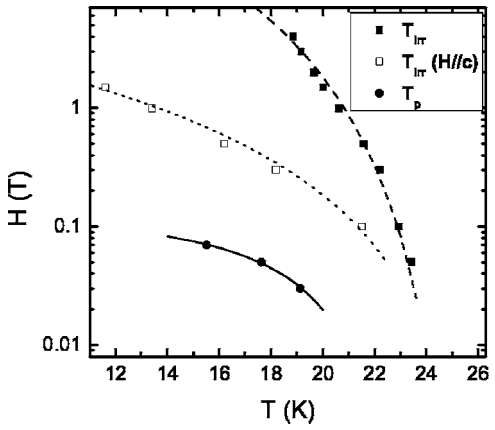

FIG. 7. The irreversibility points T_{irr} for $H\|ab$-plane (solid squares) and $H\|c$-axis (open squres) and the peak temperatures T_p for $H\|ab$-plane (solid circles). Error bars are smaller than the symbol size. The lines are fits to the data (see text).

and defect structures is also incorrect because such model suggests a temperature independence of the transition field.[29] In some materials, the peak effect is close to a melting of the vortex lattice.[8,30] This is unlikely in PLCCO because the peak effect occurs in the irreversible phase of the vortex ensemble.

Based on energy arguments, it was suggested that there is an order-disorder transition for the vortex lattice in the presence of weak point disorder.[31–33] A unified picture describing this transition and its association with the peak effect was developed recently.[34,35] In the framework of this theory, the E_{el} dominates and a quasiordered vortex lattice (or Bragg glass) is preserved at low fields. At higher fields, due to dominance of the disorder, the interaction between the vortex and pinning centers results in the proliferation of dislocations and the Bragg glass is destructed and transformed into a disordered vortex glass. The peak effect is considered to originate from this order-disorder transition in the vortex solid, where the pinning is more effective and leads to larger critical currents in a disordered vortex glass. The onset of the second peak in some materials has been interpreted in this way.[12,25,36,37]

The observed peak effect may be ascribed to a disorder-induced transition in the vortex solid. In other words, the line of T_p in Fig. 7 may separate a low-field quasiordered vortex lattice from a high-field disordered glass phase. For PLCCO below T_c, the E_{th} is expected to be insignificant and it is mainly the competition of E_{pin} and E_{el} governing the vortex structure. According to the above model, the match of these two energies marks the occurrence of the peak effect. Specifically, by equating the E_{el} with E_{pin} and considering the δT_c pinning, Giller *et al.*[12] have derived the transition field H_{on} which has a temperature dependence of the form $H_{on}(T)=H_{on}(0)[1-(T/T_c)^4]^{3/2}$. The onset of the second peak in NCCO (Refs. 12 and 25) and (Bi,Pb)2212 (Ref. 37) crystals for $H\|c$-axis can be fitted well by this equation. We find that this function also gives a nice fit to T_p, shown as the solid line in Fig. 7, with $H_{on}(0)=0.1$ T and $T_c=22$ K. The value of $H_{on}(0)$ is consistent with the disappearance of the peak effect in $H_{dc}=0.1$ T. In addition, the H_{on} is determined by the microscopic parameters such as the coherence length ξ, the penetration depth λ and the disorder parameter γ which enter the expression of E_{el} and E_{pin}.[12] In our experiments, the peak effect is revealed in constant dc fields by sweeping temperature. So it is actually triggered by the temperature dependence of those superconducting parameters.

Note that, while the above scenario appears plausible, a key feature of Josephson vortices, namely the presence of intrinsic pinning, is not involved in it since it is originally proposed for $H\|c$-axis. For $H\|ab$-plane, theory suggests that, due to the intrinsic pinning effect, Josephson vortices actually show qualitatively new features in the phase diagram compared with pancake vortices. In the absence of disorder, a pinned smectic state is predicted for Josephson vortices, which is followed by a vortex crystal at low temperature.[38,39] Furthermore, with varying the magnitude of the applied field and for slight field misalignment, both incommensurate (with the periodicity of the layered structure) and tilted smectic and crystalline phases appear. It is worthy to note that while the above phases (except for the commensurate smectic phase) may be rendered glassy in the presence of weak point disorder, the nature of the resulting phases is yet unclear.[38] Thus, under this circumstance, one may doubt whether it is still appropriate to associate the observed peak effect with a possible disorder-induced transition in Josephson vortices. Indeed, in our crystal, though the peak effect is observed for the $H\|ab$-plane, one is unable to detect its occurrence for $H\|c$-axis at similar measured conditions. This suggests that certain characteristics unique to Josephson vortices may be crucial to the appearance of the peak effect for the $H\|ab$-plane. Clearly, further experimental work and more detailed theory than available are called for to elucidate what underlies the observed results.

IV. SUMMARY

We have made a comparison of the ac susceptibility in PLCCO between $H\|ab$-plane and $H\|c$-axis. while the sample shows a linear response at low temperature for $H\|c$-axis, it enters into a bulk critical state for $H\|ab$-plane at the similar measured condition. For $H\|ab$-plane, the dip in $\chi'(T)$ signifies the existence of peak effect due to Josephson vortices. The temperature at which the peak effect manifests decreases with increasing fields. Though a scenario based on a disorder-induced transition in the vortex solid is proposed to account for this peak effect, its underlying origin needs to be clarified in the future. These findings should stimulate further theoretical and experimental explorations of the Josephson vortex matter in this system.

ACKNOWLEDGMENTS

This work is supported by the National Science Foundation of China, the Ministry of Science and Technology of China (973 project: Contract No. 2006CB01002), the CAS project ITSCNEM. Pengcheng Dai is supported by the U. S. NSF Grant No. DMR-0453804. One of the authors (O.R.N.L.) is supported by DOE Contract No. DE-AC05-00OR22725 with UT/Battelle, LLC.

*Electronic address: hhwen@aphy.iphy.ac.cn

[1] M. Pissas, S. Lee, A. Yamamoto, and S. Tajima, Phys. Rev. Lett. **89**, 097002 (2002).
[2] S. R. Park, S. M. Choi, D. C. Dender, J. W. Lynn, and X. S. Ling, Phys. Rev. Lett. **91**, 167003 (2003).
[3] M. J. Higgins and S. Bhattacharya, Physica C **257**, 232 (1996).
[4] N. Kokubo, K. Kadowaki, and K. Takita, Phys. Rev. Lett. **95**, 177005 (2005).
[5] S. S. Banerjee, N. G. Patil, S. Saha, S. Ramakrishnan, A. K. Grover, S. Bhattacharya, G. Ravikumar, P. K. Mishra, T. V. Chandrasekhar Rao, V. C. Sahni, M. J. Higgins, E. Yamamoto, Y. Haga, M. Hedo, Y. Inada, and Y. Onuki, Phys. Rev. B **58**, 995 (1998).
[6] B. Khaykovich, E. Zeldov, D. Majer, T. W. Li, P. H. Kes, and M. Konczykowski, Phys. Rev. Lett. **76**, 2555 (1996).
[7] K. Deligiannis, P. A. J. de Groot, M. Oussena, S. Pinfold, R. Langan, R. Gagnon, and L. Taillefer, Phys. Rev. Lett. **79**, 2121 (1997).
[8] J. Shi, X. S. Ling, R. Liang, D. A. Bonn, and W. N. Hardy, Phys. Rev. B **60**, R12593 (1999).
[9] G. Blatter, M. V. Feigel'man, V. B. Geshkenbein, A. I. Larkin, and V. M. Vinokur, Rev. Mod. Phys. **66**, 1125 (1994).
[10] V. F. Correa, G. Nieva, and F. de la Cruz, Phys. Rev. Lett. **87**, 057003 (2001).
[11] Y. Hidaka and M. Suzuki, Nature (London) **338**, 635 (1989); C. Marcenat, R. Calemczuk, A. F. Khoder, E. Bonjour, C. Marin, and J. Y. Henry, Physica C **216**, 443 (1993).
[12] D. Giller, A. Shaulov, R. Prozorov, Y. Abulafia, Y. Wolfus, L. Burlachkov, Y. Yeshurun, E. Zeldov, V. M. Vinokur, J. L. Peng, and R. L. Greene, Phys. Rev. Lett. **79**, 2542 (1997).
[13] M. Matsuura, Pengcheng Dai, H. J. Kang, J. W. Lynn, D. N. Argyriou, K. Prokes, Y. Onose, and Y. Tokura, Phys. Rev. B **68**, 144503 (2003).
[14] H. J. Kang, Pengcheng Dai, H. A. Mook, D. N. Argyriou, V. Sikolenko, J. W. Lynn, Y. Kurita, S. Komiya, and Y. Ando, Phys. Rev. B **71**, 214512 (2005).
[15] M. Tachiki and S. Takahashi, Solid State Commun. **70**, 291 (1989).
[16] Y. Wang, S. L. Li, P. Dai, and H. H. Wen (unpublished).
[17] V. B. Geshkenbein, V. M. Vinokur, and R. Fehrenbacher, Phys. Rev. B **43**, R3748 (1991).
[18] C. P. Bean, Phys. Rev. Lett. **8**, 250 (1962).
[19] F. Gömöry, Supercond. Sci. Technol. **10**, 523 (1997).
[20] X. S. Ling and J. I. Budnick, in *Magnetic Susceptibility of Superconductors and Other Spin Systems*, edited by R. A. Hein, T. L. Francavilla, and D. H. Liebenberg (Plenum, New York, 1991), p. 377.
[21] T. Ishida, K. Okuda, and H. Asaoka, Phys. Rev. B **56**, 5128 (1997).
[22] X. S. Ling, J. I. Budnick, and B. W. Veal, Physica C **282-287**, 2191 (1997).
[23] J. R. Clem, in *Magnetic Susceptibility of Superconductors and Other Spin Systems*, edited by R. A. Hein, T. L. Francavilla, and D. H. Liebenberg (Plenum, New York, 1991), p. 177.
[24] G. Pasquini and V. Bekeris, Phys. Rev. B **71**, 014510 (2005); Supercond. Sci. Technol. **19**, 671 (2006).
[25] M. C. de Andrade, N. R. Dilley, F. Ruess, and M. B. Maple, Phys. Rev. B **57**, R708 (1998).
[26] A. A. Nugroho, I. M. Sutjahja, M. O. Tjia, A. A. Menovsky, F. R. de Boer, and J. J. M. Franse, Phys. Rev. B **60**, 15379 (1999).
[27] T. Tamegai, Y. Iye, I. Oguro, and K. Kishio, Physica C **213**, 33 (1993).
[28] L. I. Glazman and A. E. Koshelev, Phys. Rev. B **43**, 2835 (1991); B. Horovitz, *ibid.* **60**, R9939 (1999).
[29] R. Yoshizaki, H. Ikeda, and D. S. Jeon, Physica C **225**, 299 (1994).
[30] W. K. Kwok, J. A. Fendrich, C. J. van der Beek, and G. W. Crabtree, Phys. Rev. Lett. **73**, 2614 (1994); X. S. Ling, S. R. Park, B. A. McClain, S. M. Choi, D. C. Dender, and J. W. Lynn, *ibid.* **86**, 712 (2001).
[31] T. Giamarchi and P. Le Doussal, Phys. Rev. B **52**, 1242 (1995); **55**, 6577 (1997).
[32] D. Ertaş and D. R. Nelson, Physica C **272**, 79 (1996).
[33] V. Vinokur, B. Khaykovich, E. Zeldov, M. Konczykowski, R. A. Doyle, and P. H. Kes, Physica C **295**, 209 (1998).
[34] G. P. Mikitik and E. H. Brandt, Phys. Rev. B **64**, 184514 (2001).
[35] J. Kierfeld and V. Vinokur, Phys. Rev. B **69**, 024501 (2004).
[36] D. Giller, A. Shaulov, Y. Yeshurun, and J. Giapintzakis, Phys. Rev. B **60**, 106 (1999).
[37] Y. P. Sun, Y. Y. Hsu, B. N. Lin, H. M. Luo, and H. C. Ku, Phys. Rev. B **61**, 11301 (2000).
[38] L. Balents and D. R. Nelson, Phys. Rev. B **52**, 12951 (1995); Phys. Rev. Lett. **73**, 2618 (1994).
[39] X. Hu and M. Tachiki, Phys. Rev. Lett. **80**, 4044 (1998).